

Hidden nonreciprocity as a stabilizing effective potential in active matter

Matthew Du^{1,2,*} and Suriyanarayanan Vaikuntanathan^{1,2,†}

¹*Department of Chemistry, University of Chicago, Chicago, Illinois 60637, USA*

²*The James Franck Institute, University of Chicago, Chicago, Illinois 60637, USA*

(Dated: January 29, 2024)

Active matter with nonreciprocal interactions is known for its distinctive dynamics. To shed light on the stationary properties of such systems, we consider paradigmatic systems of nonreciprocally coupled active Ornstein-Uhlenbeck particles. For each system, we uniquely decompose the interparticle force into an energy gradient and a transverse nonconservative force. We show that the steady-state distribution of positions, which would only reflect the energy if the noise were thermal, features the transverse force as an effective potential that stabilizes the energy minima, due to the persistent noise that propels the particles. We exactly solve the distribution for nonreciprocal harmonic oscillators and numerically verify the effective stability for systems with more complex couplings. Our work suggests that energy injection at the single-particle level controls how, if at all, nonreciprocity in the interactions appears in stationary states of active matter.

Active matter is a broad category of physical systems, where particles couple to their local environment in a way that keeps them in a nonequilibrium state [1–4]. As a result, both single-particle and interparticle behaviors are quite different than in systems at equilibrium. Notably, active particles are self-propelling and can often interact nonreciprocally with each other. While the physics involving self-propulsion has been extensively studied, only recently has it been shown that active matter with nonreciprocal interactions exhibit distinctive dynamics, including oscillatory collective motion [5–7] and unidirectional energy propagation [7, 8].

The stationary properties of such a system, i.e., active systems with non-reciprocal interactions, are less clear. For example, it has been shown that breaking reciprocity in the interactions can alter the steady-state distribution of particle positions [9–13], $P(\mathbf{r})$, as well as that of the velocities [14]. However, the aforementioned dynamical features suggest that $P(\mathbf{r})$, in some cases, need not change. That is, adding nonreciprocity might simply shuffle the chronological order in which the positions are explored, without changing the proportion of time spent at each position. Furthermore, the stationary properties intrinsic to a nonreciprocal system, i.e., those that are not in reference to some reciprocal system, are not understood well, including how these properties are affected by self-propulsion.

Here, we shed light on these points by studying paradigmatic systems of nonreciprocally interacting active particles, whose interparticle force can be decomposed into the gradient of a potential and a transverse nonconservative force. We find that the transverse component, which has no effect on $P(\mathbf{r})$ under thermal noise [15] [Fig. 1(a)], has a stabilizing effect on $P(\mathbf{r})$ due to the persistent (active) noise source that drives self-propulsion [Fig. 1(b)]. For some

of the systems, we can associate the nonreciprocity with the transverse force. Thus, the nonreciprocity appears in $P(\mathbf{r})$ under the persistent noise while going undetected under thermal noise. This key result has direct implications for the inference of nonreciprocal interactions in active matter [16–18] and the engineering of such couplings to produce properties of interest [8, 19].

We demonstrate our results in the context of a nonreciprocal version of active Ornstein-Uhlenbeck particles (AOUPs) [20–24], a prototypical model of active matter. The system evolves according to overdamped dynamics,

$$\dot{\mathbf{r}} = \mathbf{F}(\mathbf{r}) + \boldsymbol{\eta}(t), \quad (1)$$

where \mathbf{r} indicates the positions of the particles. The force \mathbf{F} describes their interactions, where nonreciprocity is characterized here by

$$\frac{\partial F_i}{\partial r_j} \neq \frac{\partial F_j}{\partial r_i}, \quad i \neq j \quad (2)$$

and thus renders \mathbf{F} nonconservative. For simplicity, we assume that nonreciprocity is controlled by a single parameter α , where $\alpha \neq 0$ breaks reciprocity and $\alpha = 0$ does not. In classical mechanics, Eq. (2) implies a violation of Newton’s third law (action-reaction symmetry). Representing environmental fluctuations while also propelling the particles, $\boldsymbol{\eta}$ is a persistent Gaussian noise defined by ($k_B = 1$)

$$\langle \eta_i(t) \rangle = 0, \quad (3a)$$

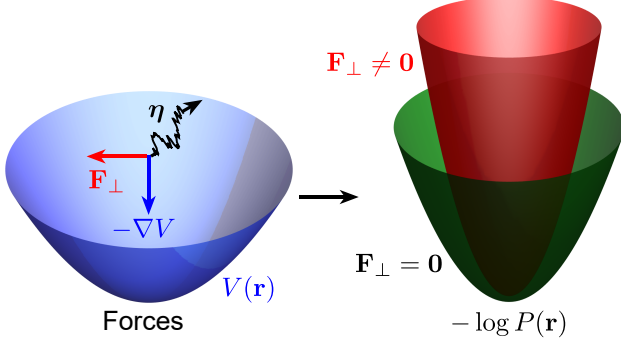
$$\langle \eta_i(t) \eta_j(t') \rangle = \frac{T}{\tau} \delta_{ij} e^{-|t-t'|/\tau}, \quad (3b)$$

where T controls the noise strength and τ is the persistence time. Hereafter, we refer to $\boldsymbol{\eta}$ with statistics (3) as persistent noise. For comparison purposes, we also consider the limit $\tau \rightarrow 0$, in which $\boldsymbol{\eta}$ reduces to thermal noise, which has zero mean [Eq. (3a)] and no temporal correlations, $\langle \eta_i(t) \eta_j(t') \rangle = 2T \delta_{ij} \delta(t-t')$.

* madu@uchicago.edu

† svaikunt@uchicago.edu

(a) Nonreciprocal interactions, persistent noise



(b) Nonreciprocal interactions, thermal noise

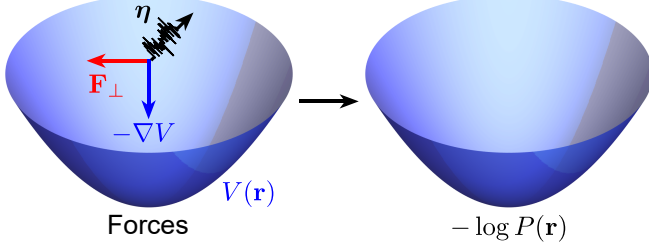


FIG. 1. Schematic illustration of the steady-state distribution of positions $P(\mathbf{r})$ of nonreciprocally interacting active Ornstein-Uhlenbeck particles whose interparticle force can be uniquely decomposed into the gradient (blue arrow) of a potential $V(\mathbf{r})$ (blue paraboloid) and a nonconservative force $\mathbf{F}_\perp(\mathbf{r})$ (red arrow) that is transverse to the energy gradient and has zero divergence. For some of the systems studied in this work, nonreciprocity can be viewed as giving rise to \mathbf{F}_\perp while leaving V unchanged. (a) Due to the persistent noise, \mathbf{F}_\perp appears in $P(\mathbf{r})$ as an effective energy correction that stabilizes the system at the minima of V . (b) If, instead, the noise were thermal, then $P(\mathbf{r})$ would be the Boltzmann distribution determined by V , i.e., would not depend on \mathbf{F}_\perp . In (a) and (b), the noise (η) is represented by a black arrow.

Before fully defining the class of systems central to this work, we begin with an example: a spring-mass chain where the springs nonreciprocally couple neighboring masses [Fig. 2(a)] [8]. Mass $i = 1, \dots, N$ experiences a force

$$F_i = - \sum_{s=\pm 1} (k - s\alpha)(r_i - r_{i+s}), \quad (4)$$

where r_i is the displacement of mass i from its rest position, and periodic boundary conditions are imposed as $r_{N+1} \equiv r_1$ and $r_0 \equiv r_N$. For the spring joining masses i and $i+1$, the displacement from rest length is $\Delta l_{i+1,i} = r_{i+1} - r_i$. The nonreciprocity of the interactions can be understood as a violation of Newton's third law: mass i acts on mass $i+1$ with force constant $k + \alpha$, but mass $i+1$ reacts to mass i with force constant $k - \alpha$.

Fig. 2(b) shows the $P(\mathbf{r})$ determined from simulations [25]. Under thermal noise, nonreciprocal ($\alpha \neq 0$) and reciprocal ($\alpha = 0$) springs have the same steady-state distribution of displacements from rest length.

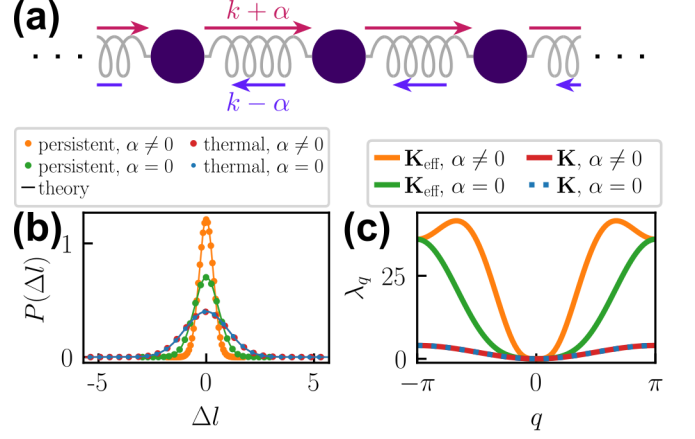


FIG. 2. Nonreciprocal spring-mass chain. (a) Schematic diagram. (b) Steady-state distribution $[P(\Delta l)]$ of displacements of the springs from their rest length (Δl) for various noise types and values of nonreciprocity parameter (α). Each set of simulated values (points of a given color) is overlaid by the corresponding theoretical values (line of the same color). (c) Eigenvalues (λ_q), indexed by wavenumber (q), of the (effective) force constant matrix governing $P(\mathbf{r})$ for various noise types [persistent (\mathbf{K}_{eff}), thermal (\mathbf{K})] and values of α . In (b)-(c), the parameters are $N = 100$, $k = 1$, $\alpha = 0, 2$, $T = 1$, and $\tau = 2$.

When switching to persistent noise, each type of spring effectively stiffens. However, the nonreciprocal springs now have smaller displacements than reciprocal springs. Thus, persistent noise enables nonreciprocity to not only modify the length of the springs at steady state but also stabilize the springs at their rest configurations.

Motivated by this intriguing interplay between nonreciprocity and noise, we formally define the class of systems to which the above example belongs. For these systems, the force \mathbf{F} can be uniquely decomposed as [15]

$$\mathbf{F} = -\nabla V + \mathbf{F}_\perp, \quad (5)$$

where $-\nabla V$ is a conservative force that drives the system down the potential $V(\mathbf{r})$, and $\mathbf{F}_\perp(\mathbf{r})$ is a transverse and divergence-free nonconservative force, i.e.,

$$-\nabla V \cdot \mathbf{F}_\perp = 0, \quad (6)$$

$$\nabla \cdot \mathbf{F}_\perp = 0, \quad (7)$$

respectively.

Since the force \mathbf{F} admits the normal decomposition (5)-(7), the steady-state distribution of positions under thermal noise is $P(\mathbf{r}) \propto \exp(-V/T)$ [15], the Boltzmann distribution determined by V [Fig. 1(a)]. It is intuitive that \mathbf{F}_\perp does not appear in $P(\mathbf{r})$, since it is perpendicular to the direction of descent on V .

We now focus on harmonic oscillators, where

$$\mathbf{F} = -\mathbf{C}\mathbf{r}, \quad (8)$$

\mathbf{C} is the force constant matrix, \mathbf{r} indicates the displacement of each particle from its rest position, and

nonreciprocity (2) corresponds to asymmetry $\mathbf{C} \neq \mathbf{C}^T$. In this case, as we will see, $P(\mathbf{r})$ under persistent noise is also exactly solvable. In addition, we will find (see examples below) that the intuition gained from this simple regime can remain applicable when \mathbf{F} has nonlinearities and constant terms.

For linear \mathbf{F} [Eq. (8)], the normal decomposition (5)-(7) is given by [26, 27]

$$V = \frac{1}{2} \mathbf{r}^T \mathbf{K} \mathbf{r}, \quad (9)$$

$$\mathbf{F}_\perp = -\mathbf{A} \mathbf{r}, \quad (10)$$

where \mathbf{K} is symmetric, \mathbf{A} is traceless, and $\mathbf{K}\mathbf{A}$ is antisymmetric. In general, the associated splitting, $\mathbf{C} = \mathbf{K} + \mathbf{A}$, is accomplished via eigendecomposition of \mathbf{C} [26, 28]. However, if \mathbf{C} is a normal matrix—defined as a matrix that commutes with its transpose or, equivalently, a matrix whose symmetric and antisymmetric parts commute—then $\mathbf{K} = (\mathbf{C} + \mathbf{C}^T)/2$ and $\mathbf{A} = (\mathbf{C} - \mathbf{C}^T)/2$ [27]. In the absence of nonreciprocity (2), \mathbf{C} is symmetric, and hence $\mathbf{K} = \mathbf{C}$ and $\mathbf{A} = \mathbf{0}$. Under thermal noise, $P(\mathbf{r})$ is governed by the harmonic potential V of Eq. (9).

To derive $P(\mathbf{r})$ under persistent noise, we generalize the approach of [29] to the nonconservative force \mathbf{F} of Eqs. (5)-(7). Below, we only present a summary of the derivation and the final result (see [25] for details). We start by recasting Eq. (1) as an underdamped Langevin equation. We then solve the corresponding Fokker-Planck equation for the steady-state distribution of positions and velocities. Marginalizing over velocities, we finally obtain

$$P(\mathbf{r}) \propto \exp(-V_{\text{eff}}/T), \quad (11)$$

where

$$V_{\text{eff}}(\mathbf{r}) = V + \frac{\tau}{2} |\nabla V|^2 + \frac{\tau}{2} \mathbf{F}_\perp^T \left[\mathbf{I} - (\mathbf{I} + \tau \mathbf{H}_V)^{-1} \right] \mathbf{F}_\perp \quad (12)$$

is the effective potential and \mathbf{H}_V is the Hessian of V . Plugging in the expressions for V [Eq. (9)] and \mathbf{F}_\perp [Eq. (10)], we arrive at the explicit solution

$$V_{\text{eff}} = \frac{1}{2} \mathbf{r}^T \mathbf{K}_{\text{eff}} \mathbf{r}, \quad (13)$$

where the effective force constant matrix is

$$\mathbf{K}_{\text{eff}} = \mathbf{K} + \tau \mathbf{K}^T \mathbf{K} + \tau \mathbf{A}^T \left[\mathbf{I} - (\mathbf{I} + \tau \mathbf{K})^{-1} \right] \mathbf{A}, \quad (14)$$

which is written in direct correspondence to Eq. (12).

It is instructive to examine the structure of V_{eff} [Eq. (12)]; an analogous analysis can be done with \mathbf{K}_{eff} [Eq. (14)]. The first term is the potential V , which underlies the steady-state distribution under thermal noise. Induced by persistent noise ($\tau \neq 0$) and scaling as $O(\tau)$, the second term stabilizes the system at the

energy minima (where $\nabla V = 0$) [Fig. 1, compare (a) and (b)] and is independent of \mathbf{F}_\perp . With persistent noise present, \mathbf{F}_\perp arises in the steady-state distribution via the third term, which (for small τ) goes as $O(\tau^2)$. This final contribution—which vanishes when any of τ , V , or \mathbf{F}_\perp is zero—can therefore be understood as an interplay among persistent noise and both the conservative and transverse forces.

To understand the role of the transverse force-dependent energy correction, we carry out a stability analysis of the corresponding term of \mathbf{K}_{eff} [third term of Eq. (14)]. Assuming the system is stable under thermal noise, we take \mathbf{K} to be positive semidefinite. It follows that the third term of \mathbf{K}_{eff} is positive semidefinite and, if we assume the generally true condition $\mathbf{K}\mathbf{A} \neq \mathbf{0}$, nonzero [25]. So, adding this term to the rest of \mathbf{K}_{eff} increases at least one eigenvalue of the effective force constant matrix while leaving the remaining eigenvalues unchanged [25]. Thus, the \mathbf{F}_\perp -containing contribution [Eq. (12)] serves to further stabilize the system at its energy minima [Fig. 1(b)]. More precise statements about how the eigenvalues change can be made if \mathbf{C} is normal [25] or the system has symmetries (e.g., translational invariance; see below).

We now apply the above theory to the nonreciprocal spring-mass chain with \mathbf{F} of Eq. (4). Writing $\mathbf{F} = -\mathbf{C}\mathbf{r}$ and noticing that \mathbf{C} is normal, we obtain the normal decomposition [Eq. (5), (9)-(10)] $\mathbf{C} = \mathbf{K} + \mathbf{A}$, where $K_{ij} = k(2\delta_{i,j} - \delta_{i-1,j} - \delta_{i+1,j})$ and $A_{ij} = \alpha(-\delta_{i+1,j} + \delta_{i-1,j})$ determine V and \mathbf{F}_\perp , respectively. It thus makes sense why nonreciprocity, controlled by α , does not affect $P(\mathbf{r})$ under thermal noise but appears in $P(\mathbf{r})$ under persistent noise as a stabilizing effective energy correction. Using the relevant (effective) force constant matrix to calculate the steady-state distribution of spring displacements under thermal (\mathbf{K}) and persistent [\mathbf{K}_{eff} , Eq. (14)] noises [25], we reproduce exactly the simulated distribution [Fig. 2(b)]. Additional agreement with the theory can be seen in how the eigenvalues of the (effective) force constant matrix change when going from thermal (\mathbf{K}) to persistent (\mathbf{K}_{eff}) noise. Indeed, Fig. 2(c) shows that, at most wavenumbers, persistent noise raises the associated eigenvalue for the reciprocal springs and even more for the nonreciprocal springs, while, at the other wavenumbers, the eigenvalues are unchanged. The changes in the eigenvalues are also consistent with the theoretical results specific to normal force constant matrices \mathbf{C} [25]. In [25], we show that, if the system size is sufficiently large ($N \gg 1$), these findings are robust to disorder and open boundary conditions.

To confirm that the above theory is exact also for nonreciprocal harmonic oscillators with non-normal force constant matrix \mathbf{C} , we choose our next example to be an experimentally relevant harmonic description of dusty plasma [30] [Fig. 3(a); see [25] for model details]. Besides \mathbf{C} not being normal, this system is different from the spring-mass chain of Eq. (4) because there are two species of masses, and the conservative part of \mathbf{F} that results from normal decomposition ($-\nabla V$) is affected

by the nonreciprocity parameter α . The last difference becomes evident, e.g., if we set $\alpha = 0$ [Fig. 3(a)], upon which the interaction between layers turns purely repulsive and thus the system turns unstable.

Fig. 3(b) shows the mean squared displacement of the springs from simulations and theory. For comparison, we also run simulations setting $\mathbf{F}_\perp = \mathbf{0}$, where the force constant matrix corresponding to \mathbf{F}_\perp [A, Eq. (10)] is obtained by numerical normal decomposition of \mathbf{C} [25, 26]. In perfect agreement with the theory, the simulations show that the transverse force does not affect the distribution of spring displacements under thermal noise but stabilizes the springs at their rest lengths under persistent noise. As the theory further predicts, the stabilizing nature of the transverse force is reflected in how the eigenvalues of the (effective) force constant matrix increase in general, and stay the same otherwise, as we switch from thermal (\mathbf{K}) to persistent noise (\mathbf{K}_{eff}) [Fig. 3(c)].

Next, we demonstrate the effective stability of the transverse force in cases where \mathbf{F} has nonlinearities. To do so, we first turn to a spin-based analog [31] of the nonreciprocal spring-mass chain (4). Specifically, we consider a nonreciprocal version of the spherical model [32] (i.e., an Ising model with continuous spin values) [Fig. 4(a)], where each spin experiences a force

$$F_i = -\mu (|\sigma|^2 - N) \sigma_i + \sum_{s=\pm 1} (J - s\alpha) \sigma_{i+s} + h, \quad (15)$$

σ is the spin vector, N is the number of spins, and the periodic boundary conditions $\sigma_{N+1} \equiv \sigma_1$ and $\sigma_0 \equiv \sigma_N$. Spin $i + 1$ experiences a force from spin i with coupling constant $J + \alpha$, while spin i feels a force from spin $i + 1$ with coupling constant $J - \alpha$. The magnetic field has strength h . In this model, the nonlinearity [first term of Eq. (15)] is a soft constraint that imposes the condition $|\sigma|^2 = N$, where $\mu > 0$ is the hardness.

Fig. 4(b)-(d) shows the simulated steady-state magnetization for ferromagnetic interaction ($J > 0$). Under thermal noise, the magnetization is unaffected by nonreciprocity ($\alpha \neq 0$), as expected by the normal decomposition of \mathbf{F} [Eq. (5)-(7)]: $V = \frac{1}{2}\mu (|\sigma|^2 - N)^2 - \sum_i J \sigma_i \sigma_{i+1} - h \sum_i \sigma_i$ and $F_{\perp,i} = \alpha(\sigma_{i+1} - \sigma_{i-1})$. In contrast, under persistent noise, nonreciprocity enhances the alignment of the spins with each other and, for $h \neq 0$, the magnetic field. Therefore, even with nonlinear \mathbf{F} , we still find that persistent noise enables nonreciprocity to stabilize energy minima. Fittingly, in the antiferromagnetic case ($J < 0$), we observe that persistent noise and nonreciprocity promote the antialignment of spins [25].

We also consider a generalization of the nonreciprocal spherical model [Eq. (15)] to two species of spins [33] [Fig. 5(a); see [25] for model details]. A key feature of this system is that the interaction between spins of different species is fully nonreciprocal.

In simulations with ferromagnetic intraspecies coupling ($J > 0$), nonreciprocity ($\alpha \neq 0$) has no effect

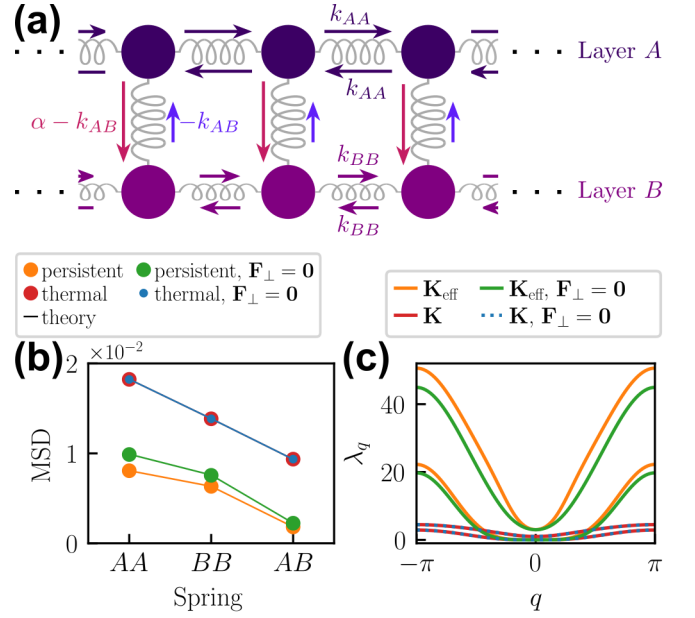


FIG. 3. Spring-mass model of dusty plasma. (a) Schematic diagram. Within layer A (B), masses are reciprocally coupled to their nearest neighbors via a spring with force constant k_{AA} (k_{BB}). In contrast, each mass of layer A behaves as if it is connected to the corresponding mass of layer B by an unstable spring with force constant $-k_{AB} < 0$, while the latter mass is effectively connected to the former mass via a stable spring with force constant $\alpha - k_{AB} > 0$. (b) Mean squared displacement (MSD) of the springs connecting masses of layer A (AA), layer B (BB), and different layers (AB) for various noise types and with or without the transverse force (\mathbf{F}_\perp). Each set of simulated values (points of a given color) is overlaid by the corresponding theoretical values (line of the same color). (c) Eigenvalues (λ_q), indexed by wavenumber (q) and further sorted into two bands, of the (effective) force constant matrix governing $P(\mathbf{r})$ for various noise types [persistent (\mathbf{K}_{eff}), thermal (\mathbf{K})] and with or without \mathbf{F}_\perp . In (b)-(c), the parameters [25] are $N = 100$, $k_{AA} = 1$, $k_{BB} = 0.6$, $k_{AB} = 1$, $\alpha = 3$, $T = 0.01$, and $\tau = 2$.

on the steady-state magnetization under thermal noise [Figs. 5(b)-(c)]. This result agrees with the normal decomposition of \mathbf{F} [25], where \mathbf{F}_\perp depends on α but V does not. Under persistent noise, though, nonreciprocity enhances the alignment of spins within each species [Figs. 5(d)-(e)].

In conclusion, we have revealed how the stationary properties of nonreciprocal AOUPs are shaped by the interplay among energy gradients, transverse forces, and self-propulsion. Specifically, the transverse forces, which would be undetectable in $P(\mathbf{r})$ if the noise were thermal, emerge in $P(\mathbf{r})$ as an effective potential that stabilizes the energy minima, due to the persistent noise propelling the particles. As a demonstration of this effect, we have shown that the breaking of reciprocity in the interactions can stiffen springs in nonreciprocal harmonic oscillators and align spins in nonreciprocal Ising-like models. In contrast, such nonreciprocity would

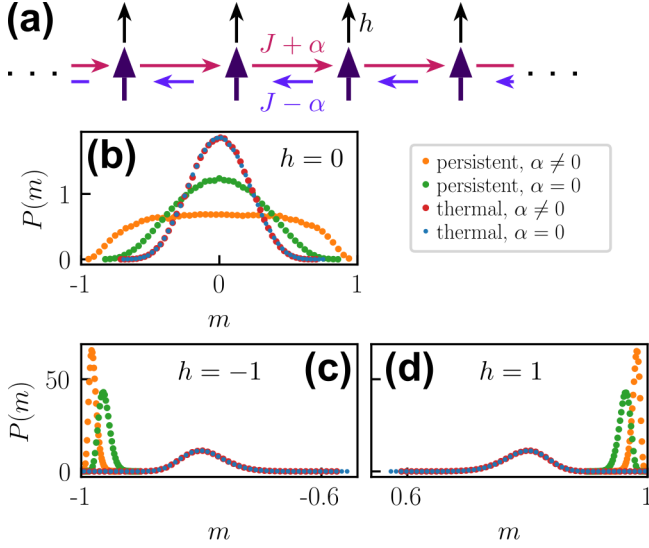


FIG. 4. Nonreciprocal spherical model. (a) Schematic diagram. (b-d) Steady-state distribution $[P(m)]$ of the magnetization (m) under persistent and thermal noise, for various values of the nonreciprocity parameter ($\alpha = 0, 2$), and for magnetic field strength (b) $h = 0$, (c) $h = -1$, and (d) $h = 1$. The other parameters are $N = 100$, $J = 1$, $\mu = 2$, $T = 1$, and $\tau = 2$.

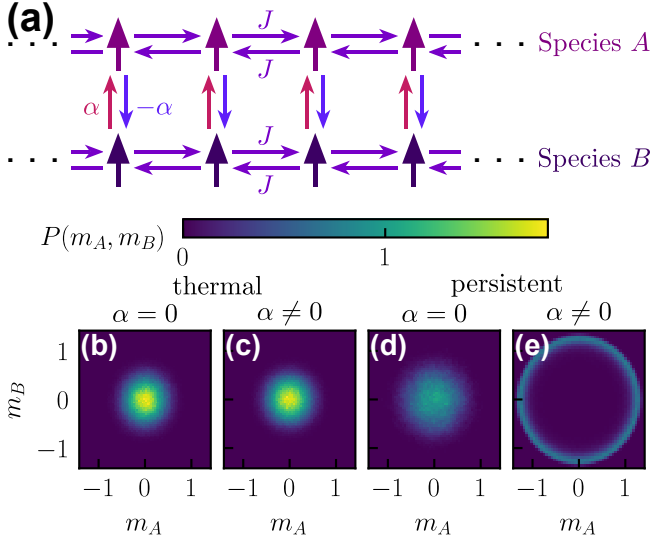


FIG. 5. Nonreciprocal spherical model with two species of spins. (a) Schematic diagram. Within each species (A, B), the spins are reciprocally coupled to their nearest neighbors with strength J . In contrast, the A (B) spins are nonreciprocally coupled to their corresponding B (A) spins with strength α ($-\alpha$). (b-e) Steady-state distribution $[P(m_A, m_B)]$ of the magnetization of A (m_A) and B (m_B) spins under thermal (b, c) and persistent (d, e) noise and for nonreciprocity parameter $\alpha = 0$ (b, d) and $\alpha = 2$ (c, e). The other parameters [25] take values $N = 100$, $J = 1$, $\mu = 2$, $T = 0.5$, and $\tau = 2$.

have no impact on $P(\mathbf{r})$ under thermal noise. Overall, our findings suggest that the consumption of energy by individual particles influences the form in which their nonreciprocal interactions appear in stationary states. Although we have focused on nonreciprocal AOUPs, we expect the results here to be relevant to other models of active particles, e.g., run-and-tumble particles [34] and Brownian particles [35]. This work provides a foundation to understand the stationary properties of active matter with nonreciprocal interactions, including neural networks [19, 36–42], colloidal particles [43, 44], and systems that exhibit flocking [12, 45–48].

ACKNOWLEDGMENTS

M. D. and S. V. are supported by DOE BES Grant No. DE-SC0019765. M. D. thanks Carlos Floyd, Akash Piya, and Daniel Seara for brainstorming sessions that led to the conception of this work; Yael Avni and Tali Khain for discussions on nonreciprocal interactions in general; Agnish Behera, Daiki Goto, Nicolas Romeo, Deb Sankar Banerjee, and Kristina Trifonova for the initial discussion of the results; Agnish Behera, Yuqing Qiu, Gregory Rassolov, and Deb Sankar Banerjee for brainstorming sessions related to active spinners, dusty plasma, and calculating the pair distribution function; Sihan Chen, Corentin Coulais, Efi Efrati, Michel Fruchart, and Vincenzo Vitelli for their critical comments and questions; Andriy Goychuk for technical discussions related to the effective potential; Nicolas Romeo for inspiring the structure of the paper; and Carlos Floyd for detailed feedback on the paper. This work was completed in part with resources provided by the University of Chicago's Research Computing Center.

[1] S. Ramaswamy, *Annu. Rev. Condens. Matter Phys.* **1**, 323 (2010).

[2] M. C. Marchetti, J. F. Joanny, S. Ramaswamy, T. B.

- Liverpool, J. Prost, M. Rao, and R. A. Simha, *Rev. Mod. Phys.* **85**, 1143 (2013).
- [3] C. Bechinger, R. Di Leonardo, H. Löwen, C. Reichhardt, G. Volpe, and G. Volpe, *Rev. Mod. Phys.* **88**, 045006 (2016).
- [4] J. O’Byrne, Y. Kafri, J. Tailleur, and F. van Wijland, *Nat. Rev. Phys.* **4**, 167 (2022).
- [5] M. Fruchart, R. Hanai, P. B. Littlewood, and V. Vitelli, *Nature* **592**, 363 (2021).
- [6] Z. You, A. Baskaran, and M. C. Marchetti, *Proc. Natl. Acad. Sci. U.S.A.* **117**, 19767 (2020), publisher: Proceedings of the National Academy of Sciences.
- [7] S. Saha, J. Agudo-Canalejo, and R. Golestanian, *Phys. Rev. X* **10**, 041009 (2020), publisher: American Physical Society.
- [8] M. Brandenbourger, X. Locsin, E. Lerner, and C. Coulais, *Nat. Commun.* **10**, 4608 (2019).
- [9] J. Bartnick, M. Heinen, A. V. Ivlev, and H. Löwen, *J. Phys.: Condens. Matter* **28**, 025102 (2015).
- [10] Y.-J. Chiu and A. K. Omar, *J. Chem. Phys.* **158**, 164903 (2023).
- [11] A. Sinha and D. Chaudhuri, *Soft Matter* **10.1039/D3SM00795B** (2024).
- [12] D. Martin, D. Seara, Y. Avni, M. Fruchart, and V. Vitelli, *An exact model for the transition to collective motion in nonreciprocal active matter* (2023).
- [13] A. Dinelli, J. O’Byrne, A. Curatolo, Y. Zhao, P. Sollich, and J. Tailleur, *Nature Communications* **14**, 7035 (2023).
- [14] A. Ivlev, J. Bartnick, M. Heinen, C.-R. Du, V. Nosenko, and H. Löwen, *Phys. Rev. X* **5**, 011035 (2015).
- [15] J. X. Zhou, M. D. S. Aliyu, E. Aurell, and S. Huang, *J. R. Soc. Interface* **9**, 3539 (2012).
- [16] X. Chen, M. Winiarski, A. Puścian, E. Knapska, A. M. Walczak, and T. Mora, *Phys. Rev. X* **13**, 041053 (2023).
- [17] V. Chardès, S. Maddu, and M. J. Shelley, *Stochastic force inference via density estimation* (2023), arXiv:2310.02366 [physics, q-bio].
- [18] W. Yu, E. Abdelaleem, I. Nemenman, and J. C. Burton, *Learning force laws in many-body systems* (2023), arXiv:2310.05273 [physics].
- [19] S. Osat and R. Golestanian, *Nat. Nanotechnol.* **1** (2022).
- [20] N. Sepúlveda, L. Petitjean, O. Cochet, E. Grasland-Mongrain, P. Silberzan, and V. Hakim, *PLoS Comput. Biol.* **9**, e1002944 (2013).
- [21] G. Szamel, *Phys. Rev. E* **90**, 012111 (2014).
- [22] N. Koumakis, C. Maggi, and R. D. Leonardo, *Soft Matter* **10**, 5695 (2014).
- [23] L. L. Bonilla, *Phys. Rev. E* **100**, 022601 (2019).
- [24] D. Martin, J. O’Byrne, M. E. Cates, E. Fodor, C. Nardini, J. Tailleur, and F. van Wijland, *Phys. Rev. E* **103**, 032607 (2021).
- [25] See Supplemental Material at [URL will be inserted by publisher] for numerical details, derivation of the effective potential, stability analysis of the effective force constant matrix, theoretical calculations for the spring-mass models, simulations of the aperiodic spring-mass chain and the antiferromagnetic spherical model, and supplemental figures, including Refs. [49-52].
- [26] C. Kwon, P. Ao, and D. J. Thouless, *Proc. Natl. Acad. Sci. U.S.A.* **102**, 13029 (2005).
- [27] J. D. Noh and J. Lee, *J. Korean Phys. Soc.* **66**, 544 (2015).
- [28] P. Ao, *Stochastic Force Defined Evolution in Dynamical Systems* (2003), arXiv:physics/0302081.
- [29] E. Fodor, C. Nardini, M. E. Cates, J. Tailleur, P. Visco, and F. van Wijland, *Phys. Rev. Lett.* **117**, 038103 (2016).
- [30] A. Melzer, V. A. Schweigert, I. V. Schweigert, A. Homann, S. Peters, and A. Piel, *Phys. Rev. E* **54**, R46 (1996).
- [31] D. S. Seara, A. Piya, and A. P. Tabatabai, *J. Stat. Mech.: Theory Exp.* **2023** (4), 043209.
- [32] T. H. Berlin and M. Kac, *Phys. Rev.* **86**, 821 (1952).
- [33] Y. Avni, M. Fruchart, D. Martin, D. Seara, and V. Vitelli, *The non-reciprocal Ising model* (2023), arXiv:2311.05471 [cond-mat, physics:nlin].
- [34] M. J. Schnitzer, *Physical Review E* **48**, 2553 (1993).
- [35] Y. Fily and M. C. Marchetti, *Phys. Rev. Lett.* **108**, 235702 (2012).
- [36] J. J. Hopfield, *Proc. Natl. Acad. Sci. U.S.A.* **79**, 2554 (1982).
- [37] J. A. Hertz, G. Grinstein, and S. A. Solla, *AIP Conference Proceedings* **151**, 212 (1986).
- [38] G. Parisi, *J. Phys. A: Math. Gen.* **19**, L675 (1986).
- [39] H. Sompolinsky and I. Kanter, *Phys. Rev. Lett.* **57**, 2861 (1986).
- [40] B. Derrida, E. Gardner, and A. Zippelius, *Europhys. Lett.* **4**, 167 (1987).
- [41] A. K. Behera, M. Rao, S. Sastry, and S. Vaikuntanathan, *Phys. Rev. X* **13**, 041043 (2023).
- [42] M. Du, A. K. Behera, and S. Vaikuntanathan, *Active oscillatory associative memory* (2023).
- [43] R. Soto and R. Golestanian, *Phys. Rev. Lett.* **112**, 068301 (2014).
- [44] J. Agudo-Canalejo and R. Golestanian, *Phys. Rev. Lett.* **123**, 018101 (2019).
- [45] D. Yllanes, M. Leoni, and M. C. Marchetti, *New J. Phys.* **19**, 103026 (2017).
- [46] Q.-s. Chen, A. Patelli, H. Chaté, Y.-q. Ma, and X.-q. Shi, *Phys. Rev. E* **96**, 020601 (2017).
- [47] L. P. Dadhichi, J. Kethapelli, R. Chajwa, S. Ramaswamy, and A. Maitra, *Phys. Rev. E* **101**, 052601 (2020).
- [48] O. Chepizhko, D. Saintillan, and F. Peruani, *Soft Matter* **17**, 3113 (2021).
- [49] C. Shi, Y.-C. Chen, X. Xiong, and P. Ao, *J. Nonlinear Math. Phys.* **30**, 834 (2023).
- [50] H. Risken and H. Risken, *Fokker-planck equation* (Springer, 1996).
- [51] A. Zee, *Quantum field theory in a nutshell*, Vol. 7 (Princeton university press, 2010).
- [52] K. M. Abadir and J. R. Magnus, *Matrix algebra*, Vol. 1 (Cambridge University Press, 2005).

Supplemental Material: Hidden nonreciprocity as a stabilizing effective potential in active matter

Matthew Du^{1,2,*} and Suriyanarayanan Vaikuntanathan^{1,2,†}

¹*Department of Chemistry, University of Chicago, Chicago, Illinois 60637, USA*

²*The James Franck Institute, University of Chicago, Chicago, Illinois 60637, USA*

(Dated: January 29, 2024)

CONTENTS

I. Numerical simulations	S1
II. Normal decomposition for non-normal force constant matrix	S2
III. Statistics of spring displacements	S2
IV. Derivation of $P(\mathbf{r})$ for nonreciprocal harmonic oscillators	S3
V. Stability analysis of \mathbf{K}_{eff}	S4
A. Proof: the second term is positive semidefinite and has nonzero trace	S4
B. Proof: the third term is positive semidefinite and has nonzero trace	S4
C. Proof: at least one eigenvalue increases while the others stay the same	S4
D. Eigenvalues: normal force constant matrix	S5
VI. Nonreciprocal spring-mass chain	S5
A. Eigendecomposition of \mathbf{K}_{eff}	S5
B. Statistics of spring displacements	S6
C. Robustness to disorder and open boundary conditions	S6
VII. Spring-mass model of dusty plasma	S6
A. Force \mathbf{F}	S6
B. Normal decomposition	S7
C. Eigendecomposition of \mathbf{K}_{eff}	S7
D. Statistics of spring displacements	S7
VIII. Nonreciprocal spherical model	S8
A. Antiferromagnetic coupling	S8
IX. Nonreciprocal spherical model with two species	S8
A. Force \mathbf{F}	S8
B. Normal decomposition	S8

I. NUMERICAL SIMULATIONS

For each system studied in this work, we simulate steady-state properties by numerically integrating equation of motion (1) using a time step of $\Delta t = 10^{-3}$. The simulations are run for 10^8 time steps. The positions of the particles (\mathbf{r}) are stored at every 200 time steps. The steady-state properties are obtained as an average over the stored positions.

* madu@uchicago.edu

† svaikunt@uchicago.edu

II. NORMAL DECOMPOSITION FOR NON-NORMAL FORCE CONSTANT MATRIX

In this section, we consider the normal decomposition of $\mathbf{F} = -\mathbf{C}\mathbf{r}$ [Eq. (8)], where \mathbf{C} is not a normal matrix. For such systems of nonreciprocal harmonic oscillators, the corresponding partitioning, $\mathbf{C} = \mathbf{K} + \mathbf{A}$, is not satisfied by letting \mathbf{K} [Eq. (9)] and \mathbf{A} [Eq. (10)] be the symmetric and antisymmetric parts of \mathbf{C} , respectively. Instead, we determine \mathbf{K} and \mathbf{A} using a procedure [26] that involves the eigendecomposition of \mathbf{C} , which we review below with some numerical details added. For non-diagonalizable \mathbf{C} , one can follow an alternative approach [26], in which \mathbf{C} is represented in Jordan normal form (see [49] for a numerical implementation of this transformation).

For diagonalizable \mathbf{C} , we can calculate \mathbf{K} and \mathbf{A} according to

$$\mathbf{K} = (\mathbf{I} + \mathbf{Q})^{-1}\mathbf{C}, \quad (\text{S1})$$

$$\mathbf{A} = \mathbf{C} - \mathbf{K} = \mathbf{Q}\mathbf{K}, \quad (\text{S2})$$

respectively, where the antisymmetric matrix \mathbf{Q} is found by solving

$$(\lambda_m + \lambda_n)\tilde{Q}_{mn} = (\lambda_m - \lambda_n)\mathbf{u}_m^T \mathbf{u}_n \quad (\text{S3})$$

for each element of $\tilde{\mathbf{Q}} = \mathbf{U}^T \mathbf{Q} \mathbf{U}$, where $\{\lambda_n\}$ are the eigenvalues of \mathbf{C} , $\{\mathbf{u}_n^T\}$ are the corresponding left (row) eigenvectors (i.e., $\mathbf{u}_n^T \mathbf{C} = \lambda_n \mathbf{u}_n^T$), and \mathbf{U}^T is the matrix whose rows are $\{\mathbf{u}_n^T\}$. If $\lambda_m + \lambda_n = 0$ for some m and n , then Eq. (S3) is an underdetermined system of equations describing $\tilde{\mathbf{Q}}$; for all such pairs m and n , we simply set $\tilde{Q}_{mn} = 0$, which satisfies the requirement that \mathbf{Q} be antisymmetric (note: the antisymmetry is preserved by the above transformations relating \mathbf{Q} and $\tilde{\mathbf{Q}}$ to each other [26], as is straightforward to show). Typically, standard methods of numerical eigendecomposition yield \mathbf{V} , the matrix whose columns are the right eigenvectors of \mathbf{C} , from which we can compute $\mathbf{U}^T = \mathbf{V}^{-1}$, where this inverse relation is guaranteed by the diagonalizability of \mathbf{C} . After solving Eq. (S3) for $\tilde{\mathbf{Q}}$, we calculate $\mathbf{Q} = \mathbf{V}\tilde{\mathbf{Q}}\mathbf{V}^T$, which yields \mathbf{K} and \mathbf{A} after plugging it in Eqs. (S1)-(S2).

III. STATISTICS OF SPRING DISPLACEMENTS

In this section, we calculate the statistics of spring displacements at steady state for harmonic oscillators moving in one dimension. Example systems include the nonreciprocal spring-mass chain [Eq. (4)] and the spring-mass model of dusty plasma [Eq. (S34)].

Let \mathbf{r} denote the displacement of the masses from their respective rest positions. For both thermal and persistent [Eqs. (11) and (13)] noise, the steady state is described by $P(\mathbf{r}) \propto \exp[-V(\mathbf{r})/T]$, where $V = \frac{1}{2}\mathbf{r}^T \mathbf{K} \mathbf{r}$ is a(n effective) potential and \mathbf{K} is a symmetric (effective) force constant matrix. We assume that the system is stable, with the eigenmodes being vibrational (positive eigenvalue and nonzero effect on spring lengths) or translational (zero eigenvalue and zero effect on spring lengths). Formally, the eigenvectors \mathbf{v}_n and corresponding eigenvalues λ_n of \mathbf{K} belong to one of two types:

$$\begin{cases} \lambda_n > 0 \text{ and } v_{ni} - v_{nj} \neq 0 \text{ for some } i, j, & \text{vibrational,} \\ \lambda_n = 0 \text{ and } v_{ni} - v_{nj} = 0 \text{ for all } i, j, & \text{translational.} \end{cases} \quad (\text{S4})$$

Applying the formula $\langle O(\mathbf{r}) \rangle = \int_{-\infty}^{\infty} d\mathbf{r} P(\mathbf{r}) O(\mathbf{r})$ for the steady-state average of observable $O(\mathbf{r})$ and making use of the eigendecomposition of \mathbf{K} [Eq. (S4)], we can calculate the statistics of the displacement of each spring from its rest length. For the spring connecting masses i and j , the average displacement $\Delta l_{i,j} \equiv r_i - r_j$ is

$$\langle \Delta l_{i,j} \rangle = 0, \quad (\text{S5})$$

and the mean squared displacement (MSD) is

$$\langle \Delta l_{i,j}^2 \rangle = T \sum_{\substack{n \\ \text{vibrational}}} \frac{(v_{ni} - v_{nj})^2}{\lambda_n}, \quad (\text{S6})$$

where the sum runs over the indices n of the vibrational eigenvectors \mathbf{v}_n [Eq. (S4)] assuming a real-valued basis. Note that the average displacement of zero [Eq. (S5)] implies that the variance of the displacement is equal to the MSD,

$$\text{Var}(\Delta l_{i,j}) = \langle \Delta l_{i,j}^2 \rangle. \quad (\text{S7})$$

In the special case where \mathbf{K} only has vibrational eigenmodes [Eq. (S4)], \mathbf{K} is invertible, and thus the MSD can be alternatively expressed as

$$\langle \Delta l_{i,j}^2 \rangle = T \left[(\mathbf{K}^{-1})_{ii} - 2(\mathbf{K}^{-1})_{ij} + (\mathbf{K}^{-1})_{jj} \right]. \quad (\text{S8})$$

IV. DERIVATION OF $P(\mathbf{r})$ FOR NONRECIPROCAL HARMONIC OSCILLATORS

In this section, we derive $P(\mathbf{r})$ [Eq. (11)] for nonreciprocal harmonic oscillators [Eq. (8)] evolving under persistent noise [Eqs. (1)-(3)]. Our approach is almost identical to the procedure of [29], except for a seemingly small difference in the ansatz for $P(\mathbf{r})$ (see below), which will turn out to be important for determining the correct dependence of $P(\mathbf{r})$ on \mathbf{F}_\perp .

The derivation begins by recasting the equation of motion (1), which describes overdamped dynamics, as an underdamped Langevin equation. To do this, we write down the equation of motion for the noise variable, an Ornstein-Uhlenbeck process given by

$$\tau \dot{\boldsymbol{\eta}} = -\boldsymbol{\eta} + \boldsymbol{\zeta}(t), \quad (\text{S9})$$

where $\boldsymbol{\zeta}$ is thermal noise with temperature T ,

$$\langle \zeta_i(t) \rangle = 0, \quad (\text{S10a})$$

$$\langle \zeta_i(t) \zeta_j(t') \rangle = 2T \delta_{ij} \delta(t - t'). \quad (\text{S10b})$$

Taking the time derivative of Eq. (1) and plugging in Eq. (S9) for $\dot{\boldsymbol{\eta}}$ yields the underdamped Langevin equation,

$$\tau \dot{\mathbf{p}} = \mathbf{F} - (\mathbf{I} - \tau \mathbf{J}_\mathbf{F}) \mathbf{p} + \boldsymbol{\zeta}(t), \quad (\text{S11})$$

where $\mathbf{J}_\mathbf{F}$ is the Jacobian of \mathbf{F} , \mathbf{I} is the identity matrix, and $\mathbf{p} = \dot{\mathbf{r}}$ are the velocities.

After rescaling time as $\tilde{t} \equiv t/\sqrt{\tau}$, we convert the Langevin equation to a Fokker-Planck equation [50],

$$\dot{P}(\mathbf{r}, \tilde{\mathbf{p}}) = \left[-\tilde{\mathbf{p}}^T \nabla_{\mathbf{r}} - \mathbf{F}^T \nabla_{\tilde{\mathbf{p}}} + \frac{1}{\sqrt{\tau}} \nabla_{\tilde{\mathbf{p}}} \cdot (\tilde{\mathbf{p}} - \tau \mathbf{J}_\mathbf{F} \tilde{\mathbf{p}}) + \frac{T}{\sqrt{\tau}} \nabla_{\tilde{\mathbf{p}}}^2 \right] P(\mathbf{r}, \tilde{\mathbf{p}}), \quad (\text{S12})$$

where $P(\mathbf{r}, \tilde{\mathbf{p}})$ is the distribution of positions and rescaled velocities $\tilde{\mathbf{p}} \equiv \sqrt{\tau} \mathbf{p}$. At steady state, the stationary distribution satisfies Eq. (S12) with the left-hand side set to zero.

To solve for the stationary distribution, consider the ansatz

$$P(\mathbf{r}, \tilde{\mathbf{p}}) \propto \exp \left[-\frac{|\tilde{\mathbf{p}}|^2}{2T} - \frac{V}{T} + \sum_{n=1}^{\infty} \tau^{n/2} \psi_n(\mathbf{r}, \tilde{\mathbf{p}}) \right], \quad (\text{S13})$$

which is similar to that of [29], except that the summation starts at $n = 1$ instead of $n = 2$, and τ can be arbitrarily large. The equation describing the stationary steady state becomes the following, which is sorted by powers of $\tau^{1/2}$:

$$\sum_{m=0}^{\infty} \tau^{m/2} \phi_m[\boldsymbol{\psi}] = 0, \quad (\text{S14})$$

where $\boldsymbol{\psi} \equiv \{\psi_n(\mathbf{r}, \tilde{\mathbf{p}})\}_{n=1}^{\infty}$ and

$$\phi_0[\boldsymbol{\psi}] = \frac{1}{T} \tilde{\mathbf{p}}^T \mathbf{F}_\perp - \tilde{\mathbf{p}}^T \nabla_{\tilde{\mathbf{p}}} \psi_1 + T \nabla_{\tilde{\mathbf{p}}}^2 \psi_1, \quad (\text{S15})$$

$$\phi_1[\boldsymbol{\psi}] = -\tilde{\mathbf{p}}^T \nabla_{\mathbf{r}} \psi_1 - \mathbf{F}^T \nabla_{\tilde{\mathbf{p}}} \psi_1 - \text{Tr} \mathbf{J}_\mathbf{F} + \frac{1}{T} \tilde{\mathbf{p}}^T \mathbf{J}_\mathbf{F}^T \tilde{\mathbf{p}} - \tilde{\mathbf{p}}^T \nabla_{\tilde{\mathbf{p}}} \psi_2 + T (\nabla_{\tilde{\mathbf{p}}} \psi_1)^T \nabla_{\tilde{\mathbf{p}}} \psi_1 + T \nabla_{\tilde{\mathbf{p}}}^2 \psi_2, \quad (\text{S16})$$

$$\begin{aligned} \phi_m[\boldsymbol{\psi}] = & -\tilde{\mathbf{p}}^T \nabla_{\mathbf{r}} \psi_m - \mathbf{F}^T \nabla_{\tilde{\mathbf{p}}} \psi_m - \tilde{\mathbf{p}}^T \mathbf{J}_\mathbf{F}^T \nabla_{\tilde{\mathbf{p}}} \psi_{m-1} \\ & - \tilde{\mathbf{p}}^T \nabla_{\tilde{\mathbf{p}}} \psi_{m+1} + T \sum_{n+n'=m+1; n, n' \geq 1} (\nabla_{\tilde{\mathbf{p}}} \psi_n)^T (\nabla_{\tilde{\mathbf{p}}} \psi_{n'}) + T \nabla_{\tilde{\mathbf{p}}}^2 \psi_{m+1}, \quad m = 2, 3, \dots \end{aligned} \quad (\text{S17})$$

Using the defining properties of \mathbf{F}_\perp [Eqs. (6)-(7)], we recursively solve the equations $\phi_m[\boldsymbol{\psi}] = 0$ for the functions $\boldsymbol{\psi}$, which results in

$$P(\mathbf{r}, \tilde{\mathbf{p}}) \propto \exp \left(-\frac{|\tilde{\mathbf{p}} - \sqrt{\tau} \mathbf{F}_\perp|^2}{2T} - \frac{V}{T} - \frac{\tau}{2T} \tilde{\mathbf{p}}^T \mathbf{H}_V \tilde{\mathbf{p}} - \frac{\tau}{2T} |\nabla_{\mathbf{r}} V|^2 \right) \quad (\text{S18})$$

as the steady-state distribution of positions and rescaled velocities. Notice that \mathbf{F}_\perp appears at $O(\sqrt{\tau})$ (to lowest order in τ), a finding that would not have been obtainable had the summation in Eq. (S13) started instead at $n = 2$ as

in [29]. In particular, \mathbf{F}_\perp shifts the velocities [Eq. (S18), first term in parentheses] and thus acts analogously to a (magnetic) vector potential.

Since the velocities are also coupled by V [Eq. (S18), first term in parentheses], the influence of \mathbf{F}_\perp persists in the marginal distribution $P(\mathbf{r})$. Indeed, integrating $P(\mathbf{r}, \mathbf{p})$ [Eq. (S18)] over all $\tilde{\mathbf{p}}$ and using the integral identity ([51], p. 15, Eq. 22)

$$\int_{-\infty}^{\infty} d\mathbf{x} \exp\left(-\frac{1}{2}\mathbf{x}^T \mathbf{M} \mathbf{x} + \mathbf{v}^T \mathbf{x}\right) = \sqrt{\frac{(2\pi)^N}{\det \mathbf{M}}} \exp\left(\frac{1}{2}\mathbf{v}^T \mathbf{M}^{-1} \mathbf{v}\right) \quad (\text{S19})$$

for matrix $\mathbf{M} \in \mathbb{R}^{N \times N}$ and vector $\mathbf{v} \in \mathbb{R}^N$, we arrive at $P(\mathbf{r})$ of Eqs. (11)-(12) in the main text.

V. STABILITY ANALYSIS OF \mathbf{K}_{eff}

In this section, we present a stability analysis of \mathbf{K}_{eff} [Eq. (14)], the effective force constant matrix that governs $P(\mathbf{r})$ under persistent noise [Eq. (3)], i.e., $\tau > 0$. We assume that \mathbf{K} [Eq. (9)], the force constant matrix governing $P(\mathbf{r})$ under thermal noise, is positive semidefinite, implying that the system is not unstable. Also, we suppose that $\mathbf{K}\mathbf{A} \neq \mathbf{0}$, which should be true in general and is used to prove that the third term of \mathbf{K}_{eff} [Eq. (14)] is nonzero.

A. Proof: the second term is positive semidefinite and has nonzero trace

The second term of \mathbf{K}_{eff} [Eq. (14)], $\mathbf{K}_{\text{eff}}^{(2)} \equiv \tau \mathbf{K}^T \mathbf{K}$, is of the form $\mathbf{M}^T \mathbf{M}$ for a matrix $\mathbf{M} \neq \mathbf{0}$. Thus, $\mathbf{K}_{\text{eff}}^{(2)}$ is positive semidefinite and $\text{tr} \mathbf{K}_{\text{eff}}^{(2)} \neq 0$ [[52], p. 214, Exercise 8.9, (a) and (b), respectively].

B. Proof: the third term is positive semidefinite and has nonzero trace

In this subsection, we prove that the third term of \mathbf{K}_{eff} [Eq. (14)], $\mathbf{K}_{\text{eff}}^{(3)} \equiv \tau \mathbf{A}^T [\mathbf{I} - (\mathbf{I} + \tau \mathbf{K})^{-1}] \mathbf{A}$, is positive semidefinite and nonzero. To do so, it is useful to write this term as

$$\mathbf{K}_{\text{eff}}^{(3)} = \mathbf{A}^T \mathbf{S} \mathbf{A}, \quad (\text{S20})$$

where we have defined

$$\mathbf{S} \equiv \tau [\mathbf{I} - (\mathbf{I} + \tau \mathbf{K})^{-1}]. \quad (\text{S21})$$

We first prove that $\mathbf{K}_{\text{eff}}^{(3)}$ is positive semidefinite. We make multiple uses of the fact that

$$\text{matrix } \mathbf{M} \text{ is positive semidefinite} \Leftrightarrow \mathbf{M} = \mathbf{M}_{1/2}^T \mathbf{M}_{1/2} \text{ for some matrix } \mathbf{M}_{1/2}. \quad (\text{S22})$$

Given the set $\{\lambda\}$ of eigenvalues of \mathbf{K} , the set of eigenvalues of \mathbf{S} is $\{\tau [1 - (1 + \tau \lambda)^{-1}]\}$ [Eq. (S21)]. So, \mathbf{S} is positive semidefinite by the positive semidefiniteness of \mathbf{K} . Using the forward direction of fact (S22), we can write $\mathbf{S} = \mathbf{S}_{1/2}^T \mathbf{S}_{1/2}$ for some matrix $\mathbf{S}_{1/2}$. Therefore, by the backward direction of fact (S22), $\mathbf{K}_{\text{eff}}^{(3)} = (\mathbf{S}_{1/2} \mathbf{A})^T (\mathbf{S}_{1/2} \mathbf{A})$ is also positive semidefinite.

Next, we prove that our assumption of $\mathbf{K}\mathbf{A} \neq \mathbf{0}$ implies $\mathbf{K}_{\text{eff}}^{(3)} \neq \mathbf{0}$. Proceeding by contradiction, we suppose that $\mathbf{K}_{\text{eff}} = \mathbf{0}$. By Eq. (S20) and the positive definiteness of \mathbf{S} , we have $\mathbf{S}\mathbf{A} = \mathbf{0}$ [[52], p. 221, Exercise 8.27(c)]. Plugging in the definition of \mathbf{S} [Eq. (S21)] and rearranging, we find $\mathbf{A} = (\mathbf{I} + \tau \mathbf{K})^{-1} \mathbf{A}$. Multiplying both sides by $\mathbf{I} + \tau \mathbf{K}$ and rearranging, we obtain $\mathbf{K}\mathbf{A} = \mathbf{0}$, a contradiction. Hence, $\mathbf{K}_{\text{eff}}^{(3)} \neq \mathbf{0}$.

Since $\mathbf{K}_{\text{eff}}^{(3)}$ is both positive semidefinite and nonzero, then $\text{tr} \mathbf{K}_{\text{eff}}^{(3)} \neq 0$ [[52], p. 214, Exercise 8.8(a)].

C. Proof: at least one eigenvalue increases while the others stay the same

Having proved that the second (Sec. VA) and third terms (Sec. VB) of \mathbf{K}_{eff} are positive semidefinite and have nonzero trace, we are ready to elucidate the effect of these terms on the eigenvalues of \mathbf{K}_{eff} . Throughout this

subsection, when we refer to the n th eigenvalue of some matrix, the index n denotes the position within an ascending (or descending) ordering of the eigenvalues.

Using the fact that the n th eigenvalue of the sum of two positive semidefinite matrices is greater than or equal to the n th eigenvalue of either matrix ([52], p. 346, Exercise 12.45), we find that the n th eigenvalue of \mathbf{K} either stays the same or increases when adding the second term of \mathbf{K}_{eff} . Similarly, the n th eigenvalue of the resulting matrix either stays the same or increases when adding the third term of \mathbf{K}_{eff} . Because of this result, along with the fact that each of the second and third terms of \mathbf{K}_{eff} has nonzero trace, at least one eigenvalue (for some n) of the (effective) force constant matrix increases upon each addition step. Thus, the effect of the second and third terms of \mathbf{K}_{eff} is to increase at least one eigenvalue while keeping the remaining eigenvalues unchanged, as stated in the main text.

D. Eigenvalues: normal force constant matrix

As mentioned in the main text, we can make more precise statements about the eigenvalues of \mathbf{K}_{eff} if the force constant matrix \mathbf{C} [Eq. (8)], which governs the dynamics, is a normal matrix. In this special case, $\mathbf{K} = (\mathbf{C} + \mathbf{C}^T)/2$ and $\mathbf{A} = (\mathbf{C} - \mathbf{C}^T)/2$ [27] are the symmetric and antisymmetric parts of \mathbf{C} . Since \mathbf{C} is normal, then $[\mathbf{K}, \mathbf{A}] = \mathbf{0}$, implying that \mathbf{K} , \mathbf{A} , and thus \mathbf{K}_{eff} [see Eq. (14)] are simultaneously diagonalizable. Let $\lambda_n(\mathbf{M})$ denote the eigenvalue of $\mathbf{M} = \mathbf{K}, \mathbf{A}, \mathbf{K}_{\text{eff}}$ associated with the n th simultaneous eigenvector (where the index n can be agnostic to the eigenvalues). Then the eigenvalues of \mathbf{K}_{eff} can be expressed in terms of those of \mathbf{K} and \mathbf{A} as

$$\lambda_n(\mathbf{K}_{\text{eff}}) = \lambda_n(\mathbf{K}) + \tau [\lambda_n(\mathbf{K})]^2 + \tau |\lambda_n(\mathbf{A})|^2 \left\{ 1 - [1 + \tau \lambda_n(\mathbf{K})]^{-1} \right\}. \quad (\text{S23})$$

From this, we deduce how noise persistence ($\tau \neq 0$) and nonzero \mathbf{F}_\perp ($\mathbf{A} \neq \mathbf{0}$) affect the eigenvalues of the (effective) force constant matrix governing $P(\mathbf{r})$:

$$\lambda_n(\mathbf{K}) = \lambda_n(\mathbf{K}_{\text{eff}})|_{\tau \neq 0, \mathbf{A} = \mathbf{0}} = \lambda_n(\mathbf{K}_{\text{eff}})|_{\tau \neq 0, \mathbf{A} \neq \mathbf{0}} \quad \text{if } \lambda_n(\mathbf{K}) = 0, \quad (\text{S24})$$

$$\lambda_n(\mathbf{K}) < \lambda_n(\mathbf{K}_{\text{eff}})|_{\tau \neq 0, \mathbf{A} = \mathbf{0}} < \lambda_n(\mathbf{K}_{\text{eff}})|_{\tau \neq 0, \mathbf{A} \neq \mathbf{0}} \quad \text{if } \lambda_n(\mathbf{K}) > 0, \lambda_n(\mathbf{A}) \neq 0, \quad (\text{S25})$$

$$\lambda_n(\mathbf{K}) < \lambda_n(\mathbf{K}_{\text{eff}})|_{\tau \neq 0, \mathbf{A} = \mathbf{0}} = \lambda_n(\mathbf{K}_{\text{eff}})|_{\tau \neq 0, \mathbf{A} \neq \mathbf{0}} \quad \text{if } \lambda_n(\mathbf{K}) > 0, \lambda_n(\mathbf{A}) = 0. \quad (\text{S26})$$

According to Eq. (S24), that the translational modes [$\lambda_n(\mathbf{K}) = 0$] are unaffected by both active noise and \mathbf{F}_\perp [through \mathbf{A} ; Eq. (10)]. In contrast, Eqs. (S25)-(S26) imply that the vibrational modes [$\lambda_n(\mathbf{K}) > 0$] are stabilized (at zero displacement) by active noise alone and, if they are not zero modes of \mathbf{A} [i.e., if $\lambda_n(\mathbf{A}) \neq 0$], further stabilized by \mathbf{F}_\perp .

VI. NONRECIPROCAL SPRING-MASS CHAIN

For the nonreciprocal spring-mass chain, with \mathbf{F} given by Eq. (4), we exactly calculate the eigenvalue spectrum of the (effective) force constant matrix, as plotted in Fig. 2(c). Using this result, we exactly calculate the steady-state distribution of the displacements of springs from their rest length, as plotted in Fig. 2(b). Below, we go through the details of these calculations.

A. Eigendecomposition of \mathbf{K}_{eff}

Since the force constant \mathbf{C} [Eq. (8)] is normal, then \mathbf{K} , \mathbf{A} , and \mathbf{K}_{eff} are simultaneously diagonalizable (Sec. VD), and the eigenvalues of \mathbf{K}_{eff} can be expressed in terms of the eigenvalues of \mathbf{K} and \mathbf{A} [Eq. (S23)]. Using $K_{ij} = k(2\delta_{i,j} - \delta_{i-1,j} - \delta_{i+1,j})$ (see main text), we see that the simultaneous eigenvectors of \mathbf{K} , \mathbf{A} , and \mathbf{K}_{eff} are the one-dimensional Fourier basis vectors $\{\mathbf{v}_q\}$, where

$$v_{qj} = \frac{1}{\sqrt{N}} e^{iqj}, \quad (\text{S27})$$

and the wavenumber q runs over all N possible values such that e^{iqN} is an N th root of unity. The corresponding eigenvalues are

$$\lambda_q(\mathbf{K}) = 2k(1 - \cos q), \quad (\text{S28a})$$

$$\lambda_q(\mathbf{A}) = 2i\alpha \sin q, \quad (\text{S28b})$$

$$\lambda_q(\mathbf{K}_{\text{eff}}) = 2k(1 - \cos q) + 4\tau k^2(1 - \cos q)^2 + 4\tau\alpha^2 \sin^2 q \left\{ 1 - [1 + 2\tau k(1 - \cos q)]^{-1} \right\}, \quad (\text{S28c})$$

where we have used Eq. (S23) in obtaining the last line. In Fig. 2(c), we plot $\lambda_q(\mathbf{K})$ and $\lambda_q(\mathbf{K}_{\text{eff}})$ as a function of q .

B. Statistics of spring displacements

Since each spring is identical, then the steady-state statistics of any one spring is equal to the respective quantities averaged over all springs. Without loss of generality, we explicitly calculate these quantities for the spring connecting masses 1 and 2, which has displacement $\Delta l_{2,1} = r_2 - r_1$. According to Eq. (S5), the displacement Δl of the springs has zero mean,

$$\langle \Delta l \rangle = 0. \quad (\text{S29})$$

Since $\mathbf{v}_{q=0}$ is a translational mode [Eq. (S4)] of \mathbf{K}_{eff} [i.e., $\lambda_{q=0}(\mathbf{K}_{\text{eff}}) = 0$], we use Eq. (S6) to compute the variance of Δl [Eq. (S7)] from the eigenvectors [Eq. (S27)]—after replacing each pair of degenerate complex eigenvectors with its corresponding pair of normalized real linear combinations—and eigenvalues [Eq. (S28)] of \mathbf{K}_{eff} :

$$\text{Var}(\Delta l) = \langle \Delta l^2 \rangle = \frac{T}{N} \sum_{q \neq 0} \frac{1}{k + 2\tau k^2(1 - \cos q) + 2\tau\alpha^2(1 + \cos q) \left\{ 1 - [1 + 2\tau k(1 - \cos q)]^{-1} \right\}}. \quad (\text{S30})$$

In Fig. 2(b), we plot the distribution of Δl as a Gaussian distribution with zero mean [Eq. (S29)] and variance given by Eq. (S30).

C. Robustness to disorder and open boundary conditions

To explore the effect of having disorder in the force constants and open boundary conditions, we consider the force [Fig. S1(a)]

$$F_i = \begin{cases} -(k_1 - \alpha_1)(r_i - r_{i+1}), & i = 1, \\ -(k_i - \alpha_i)(r_i - r_{i+1}) - (k_{i-1} + \alpha_{i-1})(r_i - r_{i-1}), & i = 2, \dots, N-1, \\ -(k_{N-1} + \alpha_{N-1})(r_N - r_{N-1}) & i = N, \end{cases} \quad (\text{S31})$$

where

$$k_i \sim U((1 - \delta)k, (1 + \delta)k) \quad (\text{S32})$$

$$\alpha_i \sim U((1 - \delta)\alpha, (1 + \delta)\alpha) \quad (\text{S33})$$

are random variables drawn from a uniform distribution on the intervals $[(1 - \delta)k, (1 + \delta)k]$ and $[(1 - \delta)\alpha, (1 + \delta)\alpha]$. Fig. S1(b)-(j) shows that as the system size (N) increases, the steady-state distribution of spring displacements becomes less affected by disorder and, in fact, converges to the corresponding distribution of the periodic analog ($\delta = 0$).

VII. SPRING-MASS MODEL OF DUSTY PLASMA

A. Force \mathbf{F}

The system consists of two spring-mass chains, which represent two vertically stacked layers of dust particles. The i th mass of each layer $l = A, B$ feels a force

$$F_{A,i} = -k_{AA} \sum_{s=\pm 1} (r_{A,i} - r_{A,i+s}) - (k_{AB})(r_{A,i} - r_{B,i}), \quad (\text{S34a})$$

$$F_{B,i} = -k_{BB} \sum_{s=\pm 1} (r_{B,i} - r_{B,i+s}) - (\alpha - k_{AB})(r_{B,i} - r_{A,i}), \quad (\text{S34b})$$

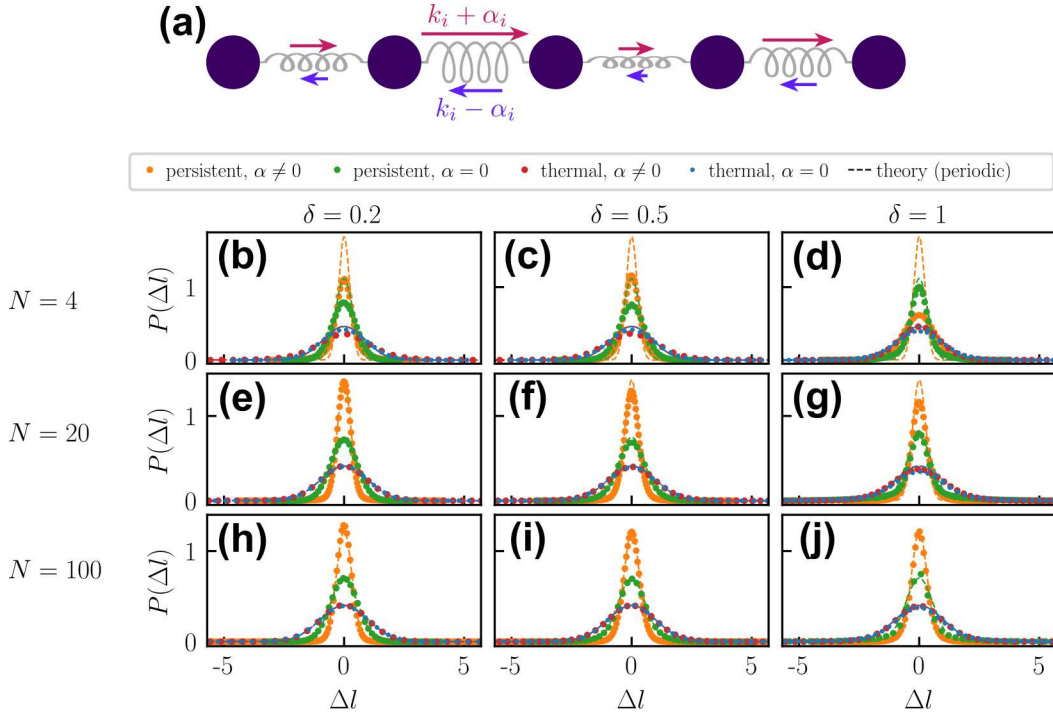


FIG. S1. Nonreciprocal spring-mass chain with disorder and open boundary conditions. (a) Schematic diagram. (b-j) Steady-state distribution $[P(\Delta l)]$ of displacements of the springs from their rest length (Δl) for various noise types and values of nonreciprocity parameter (α). These results are shown for chain lengths (b-d) $N = 4$, (e-g) $N = 20$, and (h-j) $N = 100$ and disorder strengths (b, e, h) $\delta = 0.2$, (c, f, i) $\delta = 0.5$, and (d, g, h) $\delta = 1$. Each set of simulated values (points of a given color) is calculated from a different disorder realization and overlaid by the theoretical values (dashed line of the same color) for the corresponding periodic system ($\delta = 0$). The other parameters are $k = 1$, $\alpha = 0, 2$, $T = 1$, and $\tau = 2$.

respectively, where $r_{l,i}$ is the displacement of mass i of layer l from its rest position.

B. Normal decomposition

Writing $\mathbf{F} = -\mathbf{C}\mathbf{r}$, one can show that the force constant matrix \mathbf{C} is not a normal matrix. Thus, we carry out the normal decomposition, $\mathbf{C} = \mathbf{K} + \mathbf{A}$ [Eqs. (S28)-(10)], via a procedure that involves the numerical eigendecomposition of \mathbf{C} , as reported in [26] and reviewed in Sec. II.

C. Eigendecomposition of \mathbf{K}_{eff}

The eigendecomposition of \mathbf{K}_{eff} [Eq. (14)] is carried out numerically. Due to the translational symmetry of the system and the coupling between layers [Eq. (S34) and Fig. 3(a)], each eigenvector is a superposition of Fourier mode q [Eq. (S27)] of layer A and the Fourier mode of layer B with the same wavenumber. Fig. 3(c) plots the eigenvalues versus q of their associated eigenvector.

D. Statistics of spring displacements

From Eq. (S5), the average displacement of each spring from its rest length equals zero. Using Eq. (S6), we calculate the MSD of each type of spring from the numerically computed eigenvalues and eigenvectors (Sec. VII C).

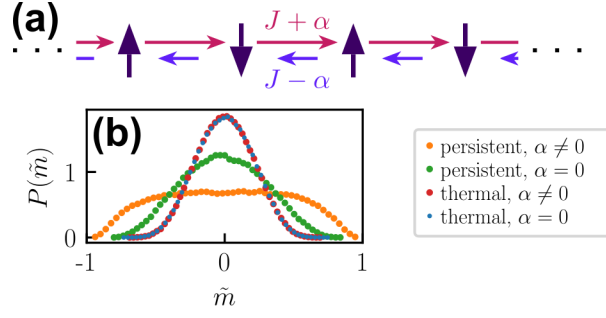


FIG. S2. Nonreciprocal spherical model with antiferromagnetic coupling. (a) Schematic diagram. (b) Steady-state distribution $[P(\tilde{m})]$ of the antimagnetization (\tilde{m}) under persistent and thermal noise, for various values of the nonreciprocity parameter ($\alpha = 0, 2$). The other parameters are $N = 100$, $J = -1$, $\mu = 2$, $T = 1$, and $\tau = 2$.

VIII. NONRECIPROCAL SPHERICAL MODEL

A. Antiferromagnetic coupling

In the main text, we explore the system with ferromagnetic coupling, $J > 0$. Fig. S2 shows the results for antiferromagnetic coupling, $J < 0$.

IX. NONRECIPROCAL SPHERICAL MODEL WITH TWO SPECIES

A. Force \mathbf{F}

The i th spin of each species $S = A, B$ feels a force

$$F_{A,i} = -\mu (|\boldsymbol{\sigma}|^2 - 2N) \sigma_{A,i} + J \sum_{s=\pm 1} \sigma_{A,i+s} + \alpha \sigma_{B,i}, \quad (\text{S35a})$$

$$F_{B,i} = -\mu (|\boldsymbol{\sigma}|^2 - 2N) \sigma_{B,i} + J \sum_{s=\pm 1} \sigma_{B,i+s} - \alpha \sigma_{A,i}, \quad (\text{S35b})$$

respectively. Similar to the previous model, $\sigma_{S,i}$ is the value of the i th spin of species S , periodic boundary conditions are defined by $\sigma_{S,N+1} \equiv \sigma_{S,1}$ and $\sigma_{S,0} \equiv \sigma_{S,N}$, $\boldsymbol{\sigma}$ is the vector of all spins, and μ is the hardness of the soft constraint that imposes the condition $|\boldsymbol{\sigma}|^2 = 2N$.

B. Normal decomposition

The normal decomposition of \mathbf{F} is given by

$$V = \frac{1}{2} \mu (|\boldsymbol{\sigma}|^2 - 2N)^2 - \sum_{S,i} J \sigma_{S,i} \sigma_{S,i+1}, \quad (\text{S36})$$

$$F_{\perp,S,i} = \alpha \times \begin{cases} \sigma_{B,i}, & S = A, \\ -\sigma_{A,i}, & S = B. \end{cases} \quad (\text{S37})$$